The Effect of Acoustic/Thermal Environments on Advanced Composite Fuselage Panels

J. Soovere*
Lockheed-California Company, Burbank, California

Described is a sonic fatigue program to determine the effect of elevated temperature on flat integrally stiffened graphite/epoxy panels. The program involved comparative sonic fatigue testing of two J-stiffened monolithic and two bladed-stiffened orthogrid panels, with one panel of each design tested at ambient temperature and the other at 254°F. The program also involved evaluation of existing analysis methods. The elevated temperature could affect the sonic fatigue life of composite panels. The higher damping in one of the panel designs is attributed to acoustic radiation. Sonic fatigue analysis methods for multimodal nonlinear panel response need to be developed.

Introduction

BECAUSE of their light weight and high fatigue resistance, graphite/epoxy composite structures offer a potential for significant weight savings over current aluminum structures. Minimum weight structures may be subjected to a combined high-acoustic/thermal environment. Such a combination of a high-thermal environment with a high-noise environment can degrade the sonic fatigue life of the composite structure.

Only limited sonic fatigue testing of stiffened composite structures has been conducted at room temperature.[1-4] No reported sonic fatigue testing of stiffened composite panels has been carried out at elevated temperatures prior to this[5] and a parallel program.[6] Limited random fatigue coupon testing has been conducted at a temperature of 180°F.[4] The temperature of the fuselage panels could, however, reach 250°F. The current sonic fatigue analysis procedure for composite panels[3] is based on a least squares fit of room temperature test data to a single-mode response theory for panels with fixed edges. The test data were obtained primarily with Z-stiffened graphite/epoxy panels. This procedure may not be applicable to composite panels in a combined acoustic/thermal environment.

The objectives of this exploratory program were to determine the effect of a high-acoustic/thermal environment on the sonic fatigue life of integrally stiffened graphite/epoxy panels and to evaluate the applicability of the existing sonic fatigue analysis method to stiffened composite panels in a high-acoustic/thermal environment.

Panel Design

The four flat integrally stiffened graphite/epoxy panels tested in this program consisted of identical pairs of J-stiffened monolithic panels (Fig. 1) and blade-stiffened orthogrid panels (Fig. 2). The J-stiffened monolithic panels were fabricated from Hercules' low resin content AS-4/3501-6 unidirectional graphite/epoxy tape. The eight-ply, 0.04 in. thick skin had a $(45°, 0°, 135°, 90°)_s$ layup. (The subscript s denotes a symmetrical layup). The 0 deg fiber direction is parallel to the short panel sides. The stiffeners, which were fabricated from graphite/epoxy tape, had a spacing of 7.1 in. in the center bay and a slightly smaller spacing in the outer bays.

In the orthogrid panels, the minisandwich skin was fabricated from Hysol's LR 100-206 unidirectional graphite/epoxy tape and the core from ADX 819 syntactic (SYNT) resin[2,4] containing glass microballoons. The six-ply, 0.055 in. thick minisandwich skin had a $(135°, 0°, 45°, SYNT)_s$ layup and a core thickness of 0.025 in. The blade stiffeners were fabricated from alternate layers of graphite/epoxy and syntactic resin, supported on either side by a three-ply thick graphite/epoxy pan. The stiffener spacing in the center bay was 10 in. The overall dimensions of the panels were 31.75×23.75 in. The edges of both panels were built up to approximately twice the skin thickness prior to curing. All of the panels were fabricated in a single cure, with cocured stiffeners.

Analysis

The panels were designed to operate in the postbuckling region with a limit and an ultimate shear load of 350 and 525 lb/in., respectively, in accordance with the criteria specified for this program. An initial shear buckling load of 100 lb/in. was selected for both panel designs since an ultimate-to-initial shear buckling ratio of 5.25 was considered practical for these panels. An anisotropic finite element program (STRAP 5), developed by Lockheed-California Company, was used to predict the initial buckling loads of 103.4 and 103 lb/in. for the monolithic and orthogrid panels, respectively. This program[7] has been shown to overestimate the initial shear buckling by approximately 3%.

The sonic fatigue design procedure[3] was used, together with the suggested correction factor for the more symmetrical J-stiffeners, to predict the sonic fatigue life of the panels at ambient temperature. The analysis indicated that an overall sound pressure level of 162-165 dB was required to fail the panels in 10 hours, well within the 167 dB capability of the acoustic progressive wave tunnel. The above dB range depended on whether the linear or nonlinear design curves in Ref. 3 were used. The orthogrid panel could sustain a 0.5 dB higher noise level than the monolithic panel for the same life, assuming equal random fatigue data and modal damping.

Modal Studies

Modal studies were conducted at ambient temperature on all of the panels and at a panel temperature of 254°F on the two elevated-temperature panels. Excitation was provided by impedance head hammer taps at each grid point on the panel. A total of 72 and 66 hammer tap locations were used on the monolithic and orthogrid panels, respectively, with five taps applied at each location. The response was measured by a noncontacting Kaman displacement transducer. The heat was sup-

Presented as Paper 83-0955 at the AIAA/ASME/ASCE/AHS 24th Structures, Structural Dynamics and Materials Conference, Lake Tahoe, Nev., May 2-4, 1983; received Oct. 11, 1983; revision received Nov. 19, 1984.

*Senior Research Specialist.

plied by six infrared lamps mounted directly above the panel. The panel temperature was measured with type P thermocouples. The temperature difference between the top of the stiffener and the skin below the stiffeners was typically 90 and 110°F for the J and blade stiffeners, respectively, at the maximum test temperature. The temperature gradient through the skin was very small.

The panel hammer tap data were analyzed with the Hewlett-Packard HP5451C Fourier analyzer to obtain modal frequencies, viscous damping ratios, and the mode shapes. The measured modal frequencies and damping ratios are summarized in Tables 1 and 2 for the monolithic and the orthogrid panels, respectively. The mode shapes measured at ambient and elevated temperatures were almost identical. Typical mode shapes for the monolithic and orthogrid panels are illustrated in Figs. 3 and 4, respectively.

The test panels were each mounted in a controlled thermal expansion test frame, developed in a research program funded by Lockheed-California Company. The test frame was insulated thermally from the test panel and the fasteners. The test frame was designed to match the thermal expansion of the panel along the edges. The biaxial static compression loads, introduced by the thermal expansion of the test panel that is now free of test frame thermal expansion effects, were primarily responsible for the fall off in the panel frequency with temperature illustrated in Figs. 5 and 6. The compression loads were due to differences in the thermal expansion of the skin panel and the frames, because of differences in the fiber orientations. Without the test frame temperature control, the subsequent rise in the test frame temperature would introduce unrepresentative tension loads into the panel, resulting in an increase in panel resonant frequencies with temperature. The elastic properties of the composite materials, and therefore the panel resonant frequencies, can also be affected by elevated temperatures. At a temperature of 250°F, the reduction in the panel resonant frequencies is expected to be less than 2% for the composite materials used in this study.

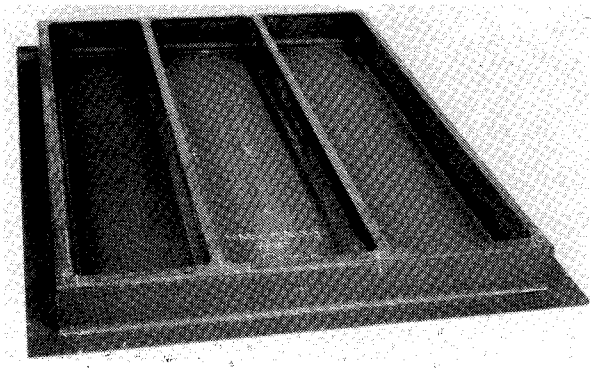

Fig. 1 J-stiffened monolithic graphite/epoxy panel.

Acoustic Radiation

The order of magnitude difference in the fundamental mode damping between the orthogrid (Table 2) and the monolithic (Table 1) panels is attributed to greater acoustic radiation from the orthogrid panels. The greater acoustic radiation is due to motion of only the large center bay in the fundamental mode (Fig. 4). This motion contrasts with the out-of-phase motion of the adjacent bays in the monolithic panel fundamental mode (Fig. 3), which produces significant cancellation[8,9] in the acoustic radiation. In the fourth panel mode, where the the cancellation effect was encountered for both panel designs, the measured viscous damping ratios are not only comparable but also very small.

The viscous damping ratio δ, due to acoustic radiation from both sides of a panel vibrating in an infinite baffle, is given approximately by[9]

$$\delta = \frac{\rho}{c}\frac{f}{\mu}\left[\int_0^a\int_0^b w(x,y)\,dx\,dy\right]^2 \Big/ \int_0^a\int_0^b w^2(x,y)\,dx\,dy$$

where ρ is the density of air, c the speed of sound in air, μ the panel mass per unit area, f the panel resonant frequency, $w(x,y)$ the corresponding mode shape, a the panel length, and b the panel width.

Table 1 Monolithic panel frequencies and viscous damping ratios

	Panel J2				Panel J1	
	Ambient		254°F		Ambient	
Mode No.	Frequency, Hz	Damping ratio	Frequency, Hz	Damping ratio	Frequency, Hz	Damping ratio
1,1	178.9	0.0058	154.1	0.0046	160.52	0.0043
2,1	262.9	0.0020	225	0.0036	243.1	0.0026
3,1	324.25	0.0025	281.9	0.0042	303.9	0.0030
4,1 (centerbay)	389.0	0.0009	341.8	0.0032	359.7	0.0026
4,1 (all bays in phase)	434.4	0.0044	388.7	0.0028	397.8	0.0089
(all bays out-of-phase)	—	—	461.1	0.0012	487.1	0.0040

Table 2 Orthogrid panel frequencies and viscous damping ratios

	Panel 01				Panel 02	
	Ambient		254°F		Ambient	
Mode No.	Frequency, Hz	Damping ratio	Frequency, Hz	Damping ratio	Frequency, Hz	Damping ratio
1,1	171.3	0.0473	159.3	0.0402	178.3	0.0393
2,1	273.2	0.0226	242.5	0.0079	273.4	0.02354
3,1	370.9	0.0015	293.7	0.0132	373.4	0.0028
4,1	460.8	0.0043	394.7	0.0034	457.5	0.0064

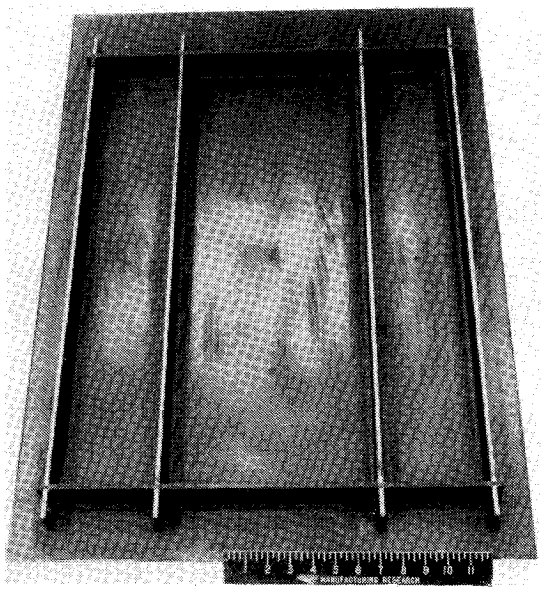

Fig. 2 Blade-stiffened orthogrid graphite/epoxy panel.

On assuming that the panel edges are simply supported, the above equation reduces to

$$\delta = \frac{64}{\pi^4} \frac{\rho}{\mu} \frac{f}{c} a\, b$$

Using this last equation and the average of the measured fundamental mode frequency for the two orthogrid panels, the acoustic radiation damping ratio is calculated at 0.0427. This value is very close to the measured damping coefficients (Table 2). In Ref. 10, acoustic radiation was also shown to provide the major part of the damping in stiffened composite honeycomb panels in the lowest modes.

Sonic Fatigue Testing

Acoustic Progressive Wave Tunnel Calibration

The test aperture in the acoustic progressive wave tunnel was blocked off with a concrete plug. Three flush-mounted microphones (at the center of the test section, opposite the test section, and at an upstream reference location), were used to measure the sound pressure level. The 300 Hz upper frequency limit of the constant-noise spectrum (Fig. 7), produced by the WYLE 3000 noise generator, was extended to approximately 450 Hz (Fig. 8) by the use of a bank of one-third octave filters. The acoustic progressive wave tunnel was then calibrated against a reference over a wide range of overall sound pressure levels. The spectrum shape was maintained over most of this range. The waviness in the noise spectrum was introduced by the crossover points of the filters. The same calibration procedure was repeated with the quartz heater panel (Fig. 9) installed in the progressive wave tunnel. The presence of the quartz heater panel did not affect the spectrum shape or level.

Test Setup and Instrumentation

A test frame and panel were mounted in the acoustic progressive wave tunnel (Fig. 10), by means of an intermediate thick plywood box, to thermally insulate the test frame from the test facility. Typically, the panel response was measured by seven strain gages, located in the center bay (Fig. 11) on all of the test panels, and a noncontacting displacement transducer (Fig. 10). Three P-type thermocouples (Fig. 11) were used to measure the panel and frame temperatures near the center of the panel. The upstream reference microphone and the microphone opposite the panel were retained to monitor the noise spectrum.

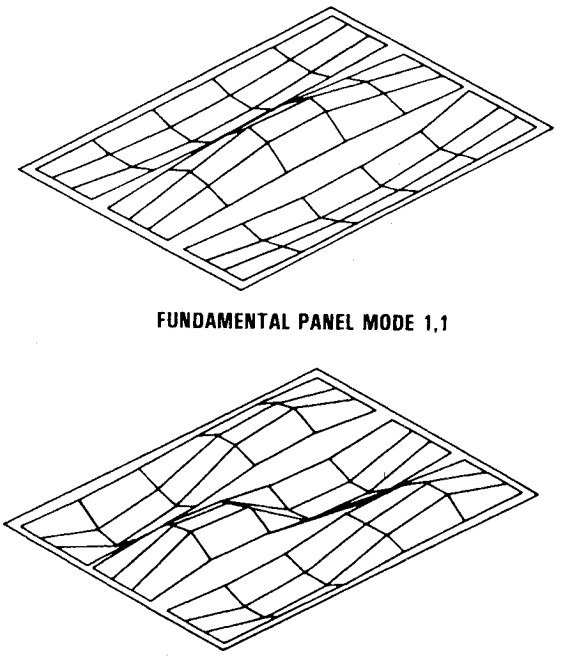

Fig. 3 Measured mode shapes for monolithic panel.

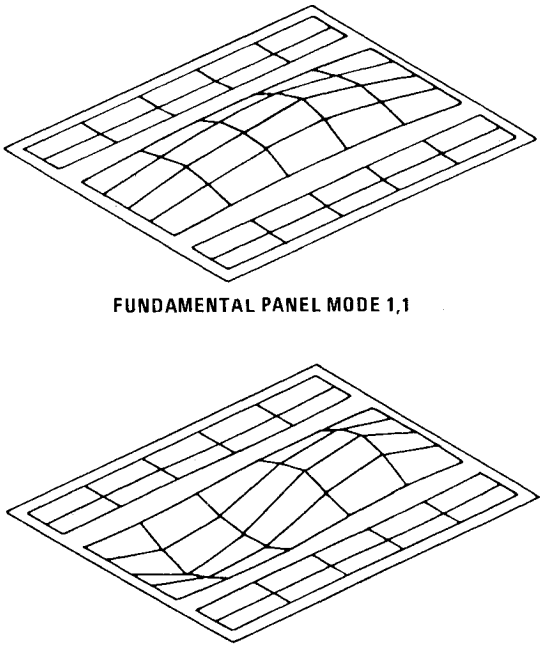

Fig. 4 Measured mode shapes for orthogrid panel.

The strain gages, microphones, and displacement transducer, after signal conditioning and amplification, were connected to a 14 channel Sangamo 3500 tape recorder. A separate monitoring channel was connected through a selector switch to an oscilloscope, DISA true rms meter, B&K 2131 digital frequency analyzer, and HP5451C Fourier analyzer. The test panel and test frame temperatures were recorded with the Fluke model 2168A digital thermometer through a selector switch.

Test Procedure

The test frame temperature, monitored by six P-type thermocouples, was set at the required temperature prior to

each day's testing. The calibration signals were recorded onto magnetic tape for all strain gages and microphone channels. The displacement transducer was initially calibrated with a vernier scale and set, thereafter, at a 0.5 in. standoff distance with an aluminum calibration block.

A strain survey was performed at a low excitation level to identify the most active strain gages. Up to four of the most active strain gages, the displacement, and the noise levels were monitored throughout the subsequent tests. Thereafter, the noise level was increased, typically in 3 dB increments, until strain gage failure or until the required test strain level was reached at the highest reading strain gage corresponding to the most critical location on the panel. The test data were recorded onto magnetic tape at each increment for subsequent analyses.

When strain gage failure occurred before reaching the required test level, a linear regression analysis was performed between the rms strain and displacement data[2,4] for the most important strain gages. The overall sound pressure level for the sonic fatigue test was subsequently set by means of the displacement transducer to a specific rms strain level, selected from available random fatigue data[1-5] at the most critical panel location.

During the sonic fatigue tests, the panels were visually inspected after 15 min, graduating to an hour or two if no visual signs of failure were detected. Also, during these tests,

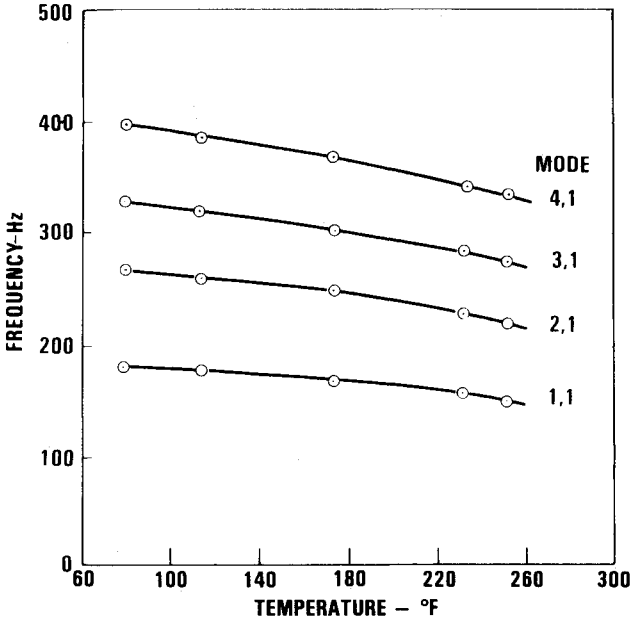

Fig. 5 Variation of modal frequencies with temperature, monolithic panel J2.

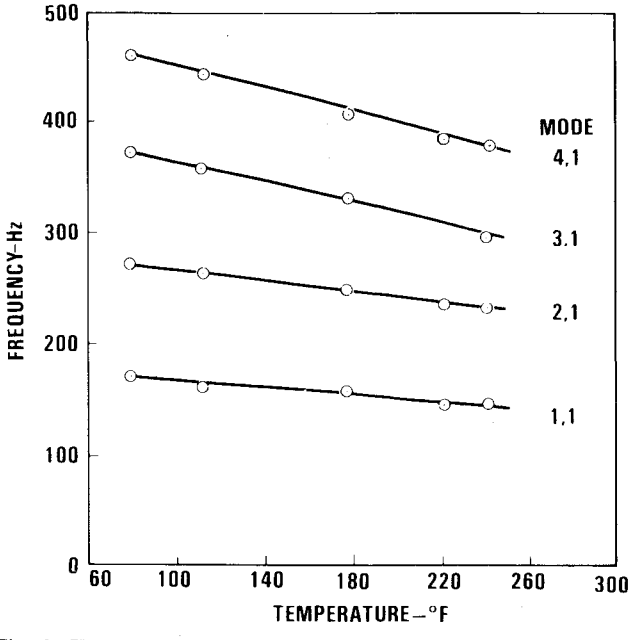

Fig. 6 Variation of modal frequencies with temperature, orthogrid panel 01.

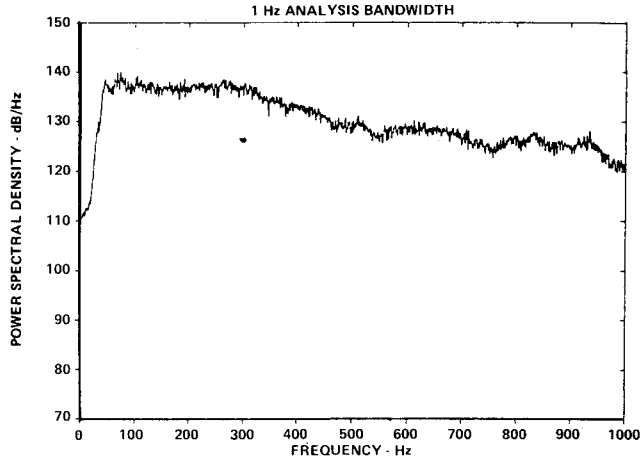

Fig. 7 Typical unshaped noise spectrum in acoustic progressive wave tunnel at test panel location.

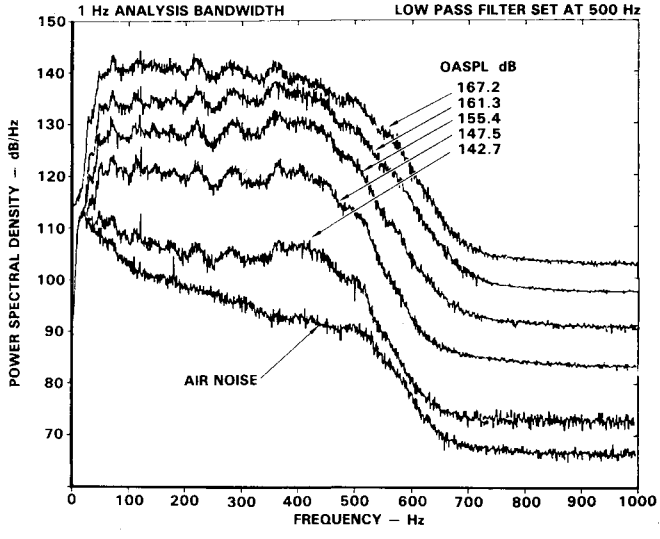

Fig. 8 Variation of random noise spectral density in the acoustic progressive wave tunnel.

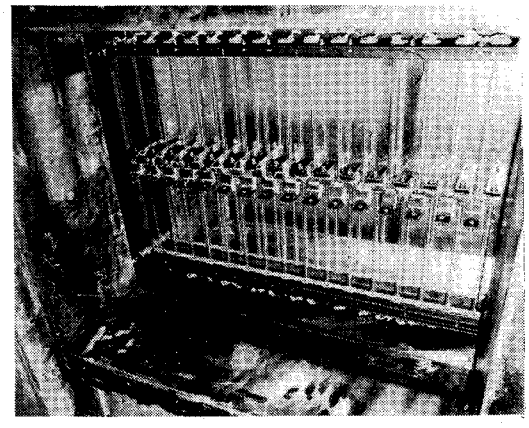

Fig. 9 Quartz heater panel mounted inside the acoustic progressive wave tunnel, opposite the test aperture.

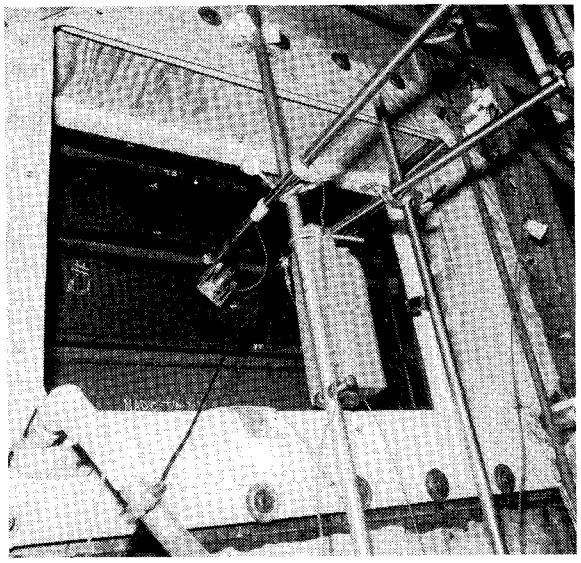

Fig. 10 Typical panel installation in acoustic progressive wave tunnel.

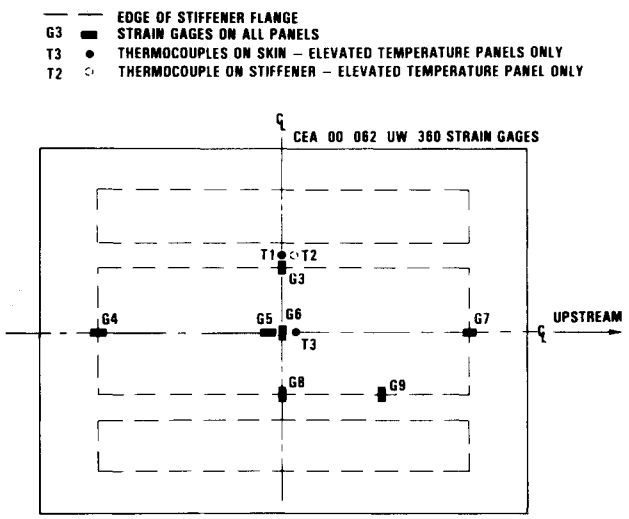

Fig. 11 Panel strain gage and thermocouple locations.

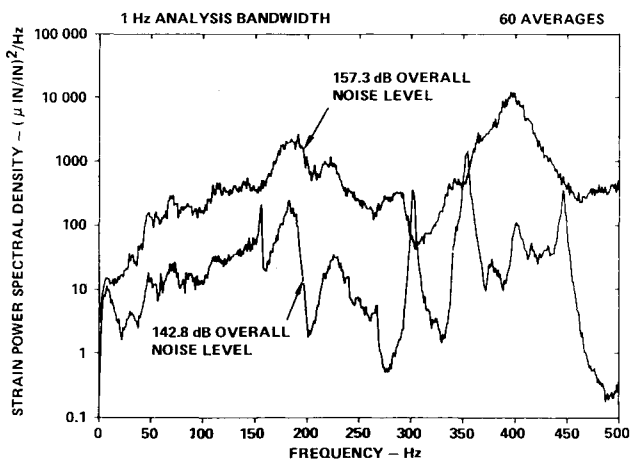

Fig. 12 Strain power spectral densities for monolithic panel J1, strain gage G8.

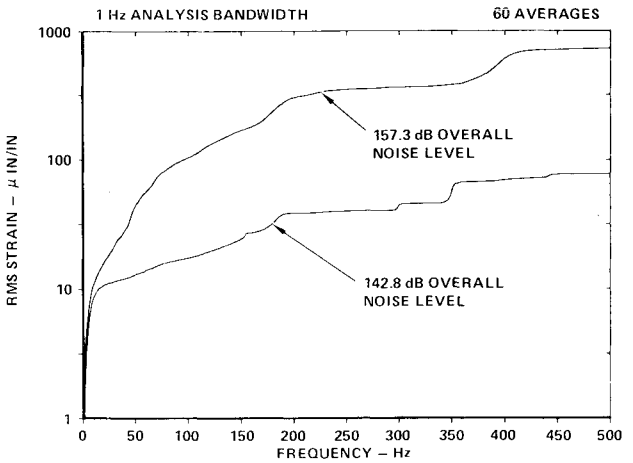

Fig. 13 Integral of the strain power spectral densities with respect to frequency, strain gage G8.

periodic narrowband analysis of the panel displacement was performed to detect any significant changes in the shape of the response spectrum. This approach is essentially the same as signature analysis. All of the data were analyzed with narrowband spectral (1 Hz) analysis using the calibration signals as reference.

The above procedure was also used on the elevated temperature test panels. However, these panels were first heated to the test temperature of 254°F with full airflow before the application of the random noise.

Test Results

The panel response at the higher noise levels was nonlinear, as can be seen by comparing the two strain spectral densities in Fig. 12. The increase in the modal frequency and the broadening of the spectral response peaks are characteristics of nonlinear response.[2,4] The contribution from each of the modes to the overall strain levels can be obtained by integrating the power spectral density with respect to the frequency,[3] as illustrated in Fig. 13. As expected, most of the contribution to the overall modes comes from the modal peaks, even for nonlinear panel vibration response.

The results of the sonic fatigue tests are summarized in Table 3. The cycles to failure were calculated from the average frequency of the spectral density response peaks, multiplied by test time. The ambient temperature J-stiffened monolithic panel failed at a higher overall sound pressure level than the elevated-temperature monolithic panel. However, the ambient-temperature orthogrid panel failed while the elevated-temperature orthogrid panel did not fail. The sonic fatigue failures in the J-stiffened monolithic panels involved the separation from the skin of one or the other of the two long frames adjacent to the center bay. Part of the skin ply, adjacent to the stiffened flange, came off with the stiffener, indicating an interlaminar type of failure within the skin. This type of failure was also obtained in the bonded graphite/epoxy panel tests described in Ref. 3. Delamination-and fracture-type failures were also obtained in the integral shear clips and stiffener end ties on one panel. In the orthogrid panel that failed, the blade stiffeners separated from the skin as a whole unit, followed by a rapid disintegration of the skin. The separation generally occurred between the first and second pan plies nearest to the skin. In some locations, part of the pan broke off at the bend radius and remained attached to the skin. The orthogrid panels contained a stress concentration at the free ends of the longest stiffeners (Fig. 2), which may have contributed to the premature failure of this panel. Fiber delaminations were observed at these locations just prior to the failure.

The rms strain levels near the center of the short panel sides were comparable to the long-side center strain levels on the monolithic panels and exceeded the long-side strain levels on the orthogrid panels. These results are due to the contributions

Table 3 Summary of sonic fatigue test results

Panel No.	Overall noise level at panel location,dB	Noise spectrum level at panel location, dB/Hz	Measured rms strain, μ in./in. Long side	Short side	Test time, h/min	Cycles
J1[a]	157.4	130.9	717	680	5/0	7.2×10^6
	161.0	134.5	900	850	5/0	7.2×10^6
	163.4	136.9	1300	1250	0/10[c]	2×10^5
J2[b]	158.4	131.3	460	581	5/0	5×10^6
	160.8	134.3	573	704	3/14[c]	3.2×10^6
02[a]	167.0	140.5	490	830	2/20[c]	2.94×10^6
01[b]	167.0	140.5	566	745	4/39	5.86×10^6

[a]Ambient test temperature. [b]254°F test temperature. [c]Failed in sonic fatigue.

Table 4 Comparison of measured and predicted acoustic fatigue life

		Predicted				Test			
Panel No.	Test OASPL, dB	rms strain μ in./in.	Freq, Hz	No. of cycles	No. of Hours	rms strain, μ in./in.	Freq, Hz	No. of cycles	No. of Hours
J1[a]	161.0	503	200	3.9×10^6	5.42	900	228	$>4.0\times10^6$	>5[d]
	163.4	663	200	5.2×10^5	0.72	1300	228	1.37×10^5	0.17
J2[b]	160.8	492	200	4.5×10^6	6.25	573	219	2.55×10^6	3.23
02[a]	167.0	998	151	$<2\times10^5$[c]	<0.4	490	253	2.12×10^6	2.33
01[b]	167.0	998	151	$<2\times10^5$[c]	<0.4	566	226	$>3.78\times10^6$	>4.65[d]

[a]Ambient test temperature. [b]254°F test temperature. [c]No test data in Ref. 3 below 2×10^5 cycles. [d]No failure.

from the higher-order panel modes, influenced by differences in the panel aspect ratios, face sheet fiber orientation, and panel construction.

Correlation with Analysis

The sonic fatigue analysis was repeated using the overall test sound pressure levels, fixed panel frequency, correction factor for J-stiffened panels, and highest strain levels at the center of the longest panel side as suggested in Ref. 3. The results are summarized in Table 4 together with the test data. Although the predicted and measured J-stiffened monolithic panel lives are in the same order of magnitude, the analysis method underestimated the measured strain level by almost a factor of two. The analysis method underestimated the sonic fatigue lives of the orthogrid panels by an order of magnitude and overestimated the rms strain level by a factor of two.

Differences exist in the random fatigue data between the bonded Z-stiffened panels with which the semiempirical analysis method[3] was developed and the integrally blade- and J-stiffened panels tested in this program. The latter designs are generally superior for sonic fatigue. Significant differences exist in the spectrum shape between test facilities for the same overall sound pressure level. The test data should correlate with spectrum level, if the spectrum is both flat over the significant panel response region and free of standing waves. Standing waves are a problem in all parallel-walled acoustic progressive wave tunnels.

A major part of the discrepancy is thought to be the omission of modal damping from the analysis method.[3] The damping should be measured at low excitation levels and not at levels were nonlinear panel response is encounted. The effect of damping can be examined by comparing the test results from the ambient temperature orthogrid and monolithic panels. These panels were designed to have comparable rms strain levels for the same overall sound pressure level, assuming equal damping. The viscous damping ratio for orthogrid panel 02 was 9.14 times that of monolithic panel J1. Since the rms strain is inversely proportional to the square root of the rms strain is inversely proportional to the square into a 9.6 dB difference in the rms strain level. The measured strain level in panel J1 (at 161 dB) was 1.84 times (5.3 dB) that measured in panel 02 for a noise level that was 6 dB lower. Consequently, the difference in damping between these two panels can account for 9.6 dB of the 11.3 dB difference in the corresponding rms strain levels, when referred to the same noise level.

Conclusions

The elevated temperature introduces thermal compression loads into the graphite/epoxy panels that reduce the panel frequencies, but not enough to cause panel buckling. The compression loads are introduced by the differences in the thermal expansion coefficients between the face sheet and the stiffeners because of differences in the fiber orientation.

Very low damping was measured on the monolithic panels. The damping for the orthogrid panel was an order of magnitude greater due to an increase in acoustic radiation from the large center bay. No significant change in the modal damping was obtained between room and elevated temperatures in the modal studies.

All of the test panels exhibited multimodal nonlinear panel responses in which higher-order modes appear to dominate. Consequently, nonlinear multimodal sonic fatigue analysis capability needs to be developed.

Elevated temperature could affect the sonic fatigue of composite panels, although the test results were inconclusive due to the small statistical sample. Coupon data[4] indicated that the effect of temperature, when combined with impact damage and moisture conditioning, could reduce the sonic fatigue life.

The current semiempirical sonic fatigue analysis method for stiffened composite panels[3] does not account for modal damping and is based on overall sound pressure level, which makes it difficult to use for spectrum shapes other than those used in the original test program. Although this sonic fatigue analysis method appears to produce a conservative design for the room temperature integrally stiffened panels in terms of panel life, it does not predict the rms strain levels to a better accuracy than

-50 and +100%. Consequently, considerable doubt exists regarding its applicability to stiffened graphite/epoxy panels other than bonded Z-stiffened panels. Random fatigue data and design methods should be developed for each unique stiffened panel design due to the sensitivity of sonic fatigue to design details.

References

[1]Jacobson, M. J., "Advanced Composite Joints: Design and Acoustic Fatigue Characteristic," AFFDL-TR-71-126, April 1972.

[2]Soovere, J., "Sonic Fatigue Testing of NASA L-1011 Composite Aileron," *The Shock and Vibration Bulletin,* No. 50, Pt. 4, Sept. 1980.

[3]Holehouse, I., "Sonic Fatigue Design Techniques for Advanced Composite Aircraft Structures," AFWAL-TR-80-3019, April 1980.

[4]Soovere, J., "Sonic Fatigue Testing of an Advanced Composite Aileron," *Journal of Aircraft,* Vol. 19, April 1982, p. 304-310.

[5]Soovere, J., "Effect of Acoustic, Thermal and Shear Loading on Flat Integrally Stiffened Graphite/Epoxy Fuselage Panels," NADC-78169-60, Feb. 1982.

[6]Jacobson, M. J., "Fatigue of V/STOL Composite Fuselage Panels Under Acoustic-Thermal Environments," NADC-81045-60, March 1981.

[7]Ostrom, R. B., "Post-Buckling Fatigue Behavior of Flat, Stiffened Graphite/Epoxy Panels Under Shear Loading," NADC-78137-60, May 1981.

[8]Beranck, L. L., (Ed.), *Noise and Vibration Control,* McGraw-Hill Book Co., New York, 1971, p. 290.

[9]Mead, D. J., "The Effect of Certain Damping Treatments on the Response of Idealized Aeroplane Structures Excited by Noise," AFML-TR-65-284, Jan. 1964.

[10]Soovere, J., "Dynamic Properties of Graphite Fiber Honeycomb Panels," AIAA Paper 73-326, March 1973.